

Article

Submerged Fixed Floating Structure under the Action of Surface Current

Zhen Cui ¹ , Zong-fu Fu ^{1,*}, Wen-hong Dai ¹ and Zheng-qing Lai ²

¹ College of Water Conservancy and Hydropower Engineering, Hohai University, Nanjing 210098, China; cuizhen@hhu.edu.cn (Z.C.); wdai@hhu.edu.cn (W.D.)

² Civil and Environmental Engineering, University of California Davis, Davis, CA 95616, USA; zlai@ucdavis.edu

* Correspondence: zffu@hhu.edu.cn; Tel.: +86-138-0159-3357

Received: 17 November 2017; Accepted: 23 January 2018; Published: 26 January 2018

Abstract: The implementation of floating structures has increased with the construction of new sluices for flood control. The overturning moment of floating structure and its influencing factors are the important parameters that determine the structural safety. It is essential to understand the overturning characteristics of these structures in currents. Based on hydrodynamic theory and equilibrium analysis, the hydraulic characteristics of a floating structure are discussed by means of theoretical analysis and experiments. A formula for the overturning moment is developed in terms of the time-averaged pressure on the structure. The corresponding parametric study aims to assess the effects of flow velocities, vertical positions, shape ratios and water levels on the overturning moment. The experimental results show that hydrodynamic factors have a significant influence on the overturning of the structure. Furthermore, a relationship is obtained between the overturning moment and the contributing parameters according to dimensional analysis and the linear fitting method of multidimensional ordinary least squares (OLS). The results predicted by the formula agree with the experimental results, demonstrating the potential for general applicability.

Keywords: floating structures; current water; hydrodynamic factors; overturning moment; OLS method

1. Introduction

The construction of water conservancy project is used to solve the problems of water resources, while it also produces the pollution of river, disaster of flood and the damage of natural environment and groundwater [1–4]. It is necessary to establish a water conservancy project that has little impact on the environment. Floating structures are widely used in new types of sluices in flood control, tidal power stations, pumping stations, and oil production platforms, and they have begun to play an important role as environmentally friendly facilities [5–7]. The stability of the structure is an issue of concern because such stability affects both construction and operation.

Research in recent years has focused on the stability of floating structures and the interaction between water and floating structures in infinite water, still water, and water under the action of wave motions. Roy and Ghosh [8] proposed a simple model to estimate the horizontal force and moment of a floating plate against waves at different depths and found that the force and moment converged with increasing wave period and depth. Hayatdavoodi and Seiffert [9–12] conducted laboratory experiments and numerical simulations of conoidal waves propagating over a submerged floating plate. The vertical force acting on the submerged floating plate appeared to scale linearly with the wave height, while the horizontal force varied nonlinearly with wavelength. They noted that the water depth and the wave submergence depth had an effect on the safety and that the interaction between a wave and a floating bridge contributed significantly to the force magnitude. Lee and Hong [13] adopted experimental

tests and the Marker and Cell numerical method to verify the nonlinear wave effect on a large floating structure. The test configuration reduced the wave force and improved the stability with the installation of baffles. Belibassakis and Athanassoulis [14] analyzed the hydrodynamic characteristics of the floating structure by hybrid technology in any water depths. The seabed model with different slopes and curvatures was shown to have an influence on the hydrodynamic characteristics and the response of floating structures under the action of waves. Liu et al. [15] predicted the wave force and the momentum of the structure for infinite water and finite water depths using the three-dimensional time-domain Green's function method. In addition, they investigated the motion response under the action of waves by means of numerical simulations [16,17], concluding that the water depth had an effect on the overturning phenomenon.

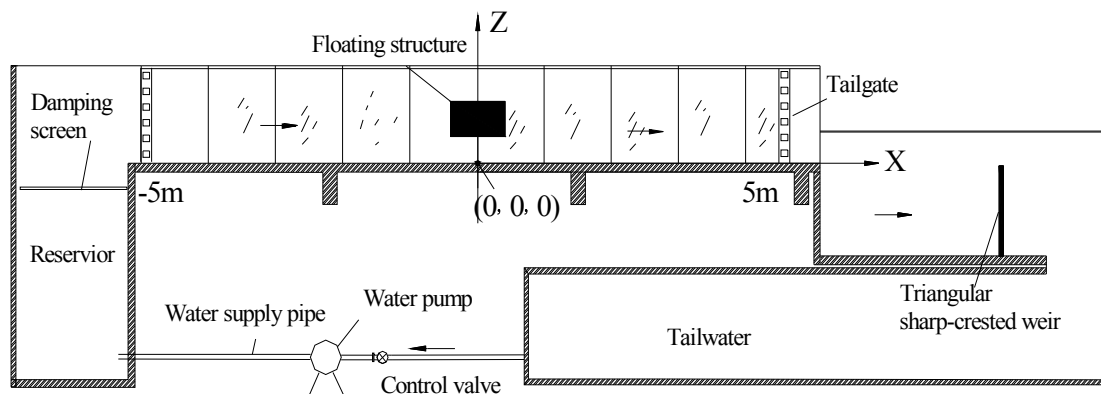
The studies noted above considered the response of floating structures in still water or under the action of waves in finite water, in which the momentum and its influencing factors were analyzed. Such structures have similar characteristics to ships, offshore platforms and sluices. However, the hydrodynamic conditions are different from that of ships in infinite waters and offshore platforms [18,19]. The force leading to the overturning of structures in currents consists of an inertia force, hydrodynamic pressure and frictional resistance. Lu [20] analyzed the stability of a floating bulkhead and its influencing factors in still and flowing water. He also compared the different characteristics between hydrostatic stability and dynamic stability and discussed improvement measures of the stability of a floating bulkhead. Based on the principle of force balancing, Fu et al. examined the actors affecting the overturning of floating bulkheads and developed a stability formula describing these structures [21]. They found that the inertia force and the hydrodynamic pressure in currents had an effect on the overturning phenomenon and proposed a method to improve bulkhead safety. Huang et al. [22] introduced a numerical simulation to study the relationships among water depths, flow velocities, closing angles and the floating bulkhead. Based on a neural network, Fan and Suo [23,24] established a database for floating transportation structure technology, which was used to calculate the stability of tidal power plates in the process of floating and sinking. This method overcomes the limitations of stability formulas and is easy to use. Johnson et al. [25] compared three models to calculate the dynamic responses of floating breakwaters under the action of waves and currents, wave heights, wave lengths and currents. Rey and Touboul [26] devised experiments of a submerged floating plate related to the currents acting on it. The current had a strong effect on the reflection coefficient and horizontal force. Karmakar and Guedes Soares [27] analyzed the bending moment and shear force on a moored finite floating elastic plate under gravity waves in the case of finite water depth, concluding that the effect of lateral pressure on the plate should not be neglected. Cui [28,29] adopted numerical simulation and experimental tests to study the force acting on the floating structures, the sensitivity of influencing factors were analyzed and the force formula was given. No uniformity of force acting on structures led to the overturning; however, the variation tendency of overturning and its influencing factors were not studied.

Previous studies have analyzed the influencing factors of the overturning of floating structures in currents and addressed the relationships between the factors and different positions. The influence of hydrodynamic pressure on the overturning of a floating structure is the motivation to develop a method to accurately calculate the overturning moment via hydrodynamic pressure. Based on a large number of hydraulic model tests, the theory of hydrodynamics and equilibrium analysis are employed to analyze the hydrodynamic factors acting on the capsized features of a floating structure at different positions in currents. The micro-integral method is used to calculate the structure's overturning moment. The hydraulic parameters, i.e., the floating ratio of the structure, water level, velocity and vertical position, are investigated to evaluate the stability through a theoretical analysis; also, the relationship between overturning and parameters is also described. In light of the experimental results, a formula of overturning moment in terms of the hydrodynamic pressure in currents is given; the results from the formula are in good agreement with the experimental tests. The findings provide a useful reference for the stability determination of floating structures.

2. Experimental Configuration and Design

2.1. Experimental Configuration

The experiments were conducted in a flume at the Hydraulic Laboratory, Hohai University. The dimensions of the flume were 10.00 m, 0.30 m, and 0.50 m (length, width, and height, respectively) and the slope of the flume was 0. The device used for the experiment has a self-circulation system, composed of a water pump, control valve, damping screen, glass flume, tailgate, triangular sharp-crested weir and tail water; Figure 1a shows the layout of the experimental rig. A damping screen was installed at the upstream of the flume to calm the flow; the testing area of the floating structure was in the center of the flume. Experiments were conducted under submerged flow flows. Floating structures in different positions were fixed with the side walls of flume, with their width perpendicular to the flume. The water flows through the upper and lower parts of structures into the downstream and cannot flow around it. The tailgate at the end was used to regulate downstream water depth. The water supply to the flume was provided through a supply pipe from the pump, with flow control provided by a valve. A triangular sharp-crested weir at the end of the flume displayed the discharge. The water depth was measured using a point gauge to an accuracy of ± 0.01 cm, level measurements were taken at a distance of 2 m from the center of the structure, and typical velocities were obtained by particle image velocimetry (PIV). Flow characteristics around the floating structure were measured along the longitudinal section. The overturning moment of the structures caused by the surface hydrodynamic pressure in current was measured and analyzed.



(a)



(b)

Figure 1. Layout of the experimental rig: (a) experimental rig; (b) main experimental rig area.

The coordinate system is Cartesian, with its origin (0, 0, 0) on the flume bottom. The X-axis is parallel to the flume, positive downstream. The Y-axis is perpendicular with the flume, with its origin in the middle of the flume. The Z-axis is vertical, positive upwards. The layout of the main experimental rig is shown in Figure 1b.

2.2. Design of Experimental Parameters and Test Layout

During the operation of floating structures in current, factors affecting overturning moment mainly include the floating structures' shape, the vertical position and the hydraulic conditions. According to the factors affecting the overturning moment in hydraulic engineering, the indoor experiments were established and the main parameters conditions were analyzed. The experiments were conducted with the width $B = 30$ cm of the floating structure perpendicular with the flume, and the structure height was $a = 10$ cm. The unit inflow discharges were $q = 0.05, 0.06, 0.07$ and 0.08 m^2/s . To study the effect of structure size, four lengths were used, namely, $L = 10, 20, 30$ and 40 cm, in the flow direction. Four flow cases with the water level difference $\Delta H = 1, 2, 3$ and 4 cm were tested, $\Delta H = H - H'$, where H and H' are the upstream and downstream water depths, respectively. Floating structures were set at four vertical positions at depths of submergence of $e = 2, 5, 10$ and 20 cm. The opening (or gap) e beneath the structure was defined as the distance from its lower edge to the flume bottom; v denoted the velocity. The hydrodynamics parameters are illustrated in Figure 2 and experimental parameters are showed in Table 1.

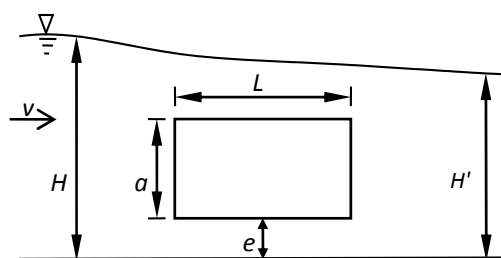


Figure 2. Schemes of the hydrodynamics parameters.

Table 1. Experimental parameters.

L (cm)	e (cm)	q ($m^2 s^{-1}$)	ΔH (cm)			
10/20/30/40	2	0.05	1.00	2.00	3.00	4.00
		0.06	1.00	2.00	3.00	4.00
		0.07	1.00	2.00	3.00	4.00
		0.08	1.00	2.00	3.00	4.00
	5	0.05	1.00	2.00	3.00	4.00
		0.06	1.00	2.00	3.00	4.00
		0.07	1.00	2.00	3.00	4.00
		0.08	1.00	2.00	3.00	4.00
	10	0.05	1.00	2.00	3.00	4.00
		0.06	1.00	2.00	3.00	4.00
		0.07	1.00	2.00	3.00	4.00
		0.08	1.00	2.00	3.00	4.00
	20	0.05	1.00	2.00	/	/
		0.06	1.00	2.00	/	/
		0.07	1.00	2.00	/	/
		0.08	1.00	2.00	/	/

The pressure distribution on the surface of the floating structures was measured using miniature dynamic pressure sensors with a resolution of 0.2 mbar. Compared with the piezometers and

other sensors, miniature dynamic pressure sensor has the benefit of high measurement precision, high-frequency and reliability, which is better to capture the pressure changes and improve the accuracy of the collection pressure. Although the flow velocity near structures is relatively large, the streamline around it is smooth, and the turbulence intensity around it is relatively weak. The change in the hydrodynamic pressure on the surface is relatively small, and the acquisition time of the sensor is 5 min. The time-averaged values were used to investigate the change. Layout of pressure measurement points is given in Figure 3.

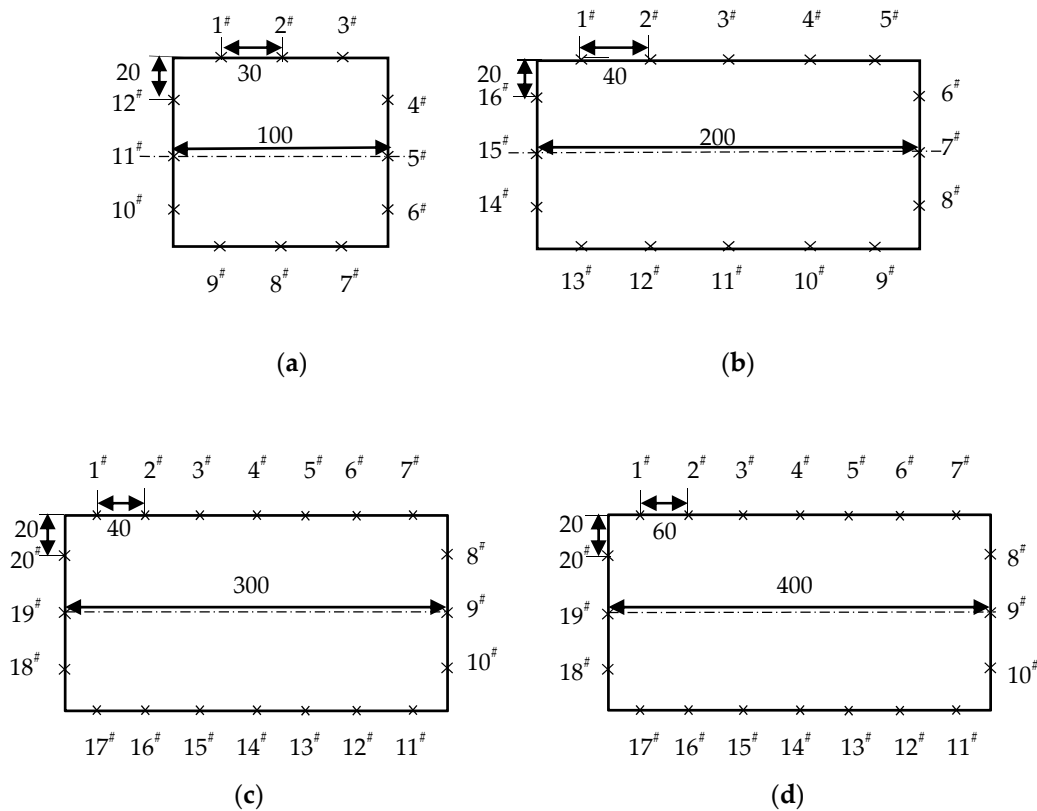


Figure 3. Layout of pressure measurement points: (a) 100 × 100; (b) 200 × 100; (c) 300 × 100; (d) 400 × 100 (mm).

3. Calculation of the Overturning Moment

The change of the hydrodynamic pressure and the distance between adjacent measuring points is relatively small; therefore, in order to get the exact value, the overturning is calculated by measuring the surface pressure using the micro-integral method. The dynamic pressure on the structure was collected, and time-averaged values were used to calculate the overturning moment by means of the micro-integral method. Figure 4 shows the calculation schematic of the overturning moment and the pressure profile of the measurements.

The upstream face of the floating structure is selected and depicted in Figure 4. The profile is parallel to the flow direction; C is the center of the floating structure. L_{i1} and L_{i2} are the horizontal distances of measuring points A and M from the measuring point to C , respectively; l is the horizontal distance from measuring points A to M , h_{i1} and h_{i2} are the water depths of the measuring points, respectively, and e_i is the pressure center of the computational domain.

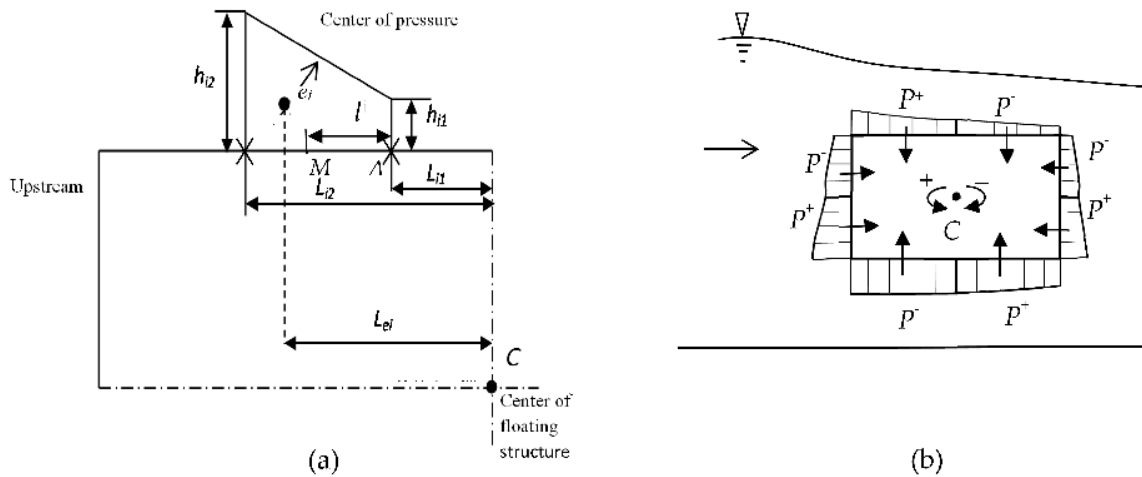


Figure 4. Calculation schematic of the overturning moment: (a) Calculation schematic; (b) Pressure profile of the measurements.

Although the flow velocity near structures is relatively large, the hydrodynamic pressure acting on the surface of the structures changes smoothly along the flow direction. The distance between adjacent measuring points is small, so it is reasonable to assume that the pressure distribution is linear between them. The pressure is calculated as follows:

$$P_i = \rho g B \int_{L_{i1}}^{L_{i2}} h(l) dl \tag{1}$$

$$h(l) = \frac{h_{i1} - h_{i2}}{L_{i1} - L_{i2}} \times l + (h_{i2} - \frac{h_{i1} - h_{i2}}{L_{i1} - L_{i2}} \times L_{i2}) \tag{2}$$

where g is the acceleration of gravity, 9.81 m/s^2 ; ρ is the water density, 1000 kg/m^3 ; dl is the differential length of M , m ; $h(l)$ is the submerged depth of M , m , and P_i is the pressure between two measuring points, N .

The distance between e_i and C is L_{ei} :

$$L_{ei} = \frac{(L_{i2} - L_{i1})(h_{i1} + 2h_{i2})}{3(h_{i1} + h_{i2})} + L_{i1} \tag{3}$$

The overturning moment in terms of the time-average pressure distribution is defined as M_{Pi} :

$$M_{Pi} = P_i L_{ei} \tag{4}$$

Therefore, the total overturning moment is calculated as follows:

$$M_P = \sum_{i=1}^n M_{Pi} \tag{5}$$

The direction of M_{Pi} is negative in the clockwise direction and positive in the counter-clockwise direction. The value of M_P is related to the unit width dynamic pressure ($B = 1 \text{ m}$).

The overturning moment of the floating structure varies according to the floating ratio of the structure, water level, velocity and vertical position based on experimental observation and analysis. Dimensional analysis is used for analyzing the relationships between influencing factors and overturning, which makes the obtained results harmonious in dimension and universal in meaning.

It found that M_P [ML^2/T^2] and the other relevant physical quantities, namely, L [L], v [L/T], g [L/T²], a [L], ΔH [L], e [L], H [L], ρ [M/L^3] and dynamic viscosity μ [MT/L^2], are related as follows:

$$f(M_P, L, v, g, \rho, a, \Delta H, e, H, \mu) = 0 \quad (6)$$

The effect of μ can be discussed in terms of the shear force. It is observed that the effect of viscosity on the floating structure can be neglected compared with the hydrodynamic pressure [29]. According to the π theorem, H , g and ρ are selected as the basic parameters. Two dimensionless Pi-groups are given: $\pi_2 = L/H$ and $\pi_4 = a/H$. The shape of floating structures is a factor that affects the overturning moment. The dimensionless parameters were rearranged logically to yield, the shape ratio to obtain: $\pi_2/\pi_4 = (L/H)/(a/H) = L/a$. The equation is derived as follows:

$$\frac{M_P}{H^4 g \rho} = F\left(\frac{L}{a}, \frac{e}{a}, \frac{v^2}{g \Delta H}, \frac{\Delta H}{a}\right) \quad (7)$$

where $\frac{L}{a}$ is the shape ratio. Given the definition of the overturning moment of floating structures' and M_{KP} , we obtain

$$\frac{v^2}{g \Delta H} = Fr^2 \frac{M_P}{H^4 g \rho} = M_{KP}$$

Thus,

$$M_{KP} = F\left(\frac{L}{a}, \frac{e}{a}, Fr^2, \frac{\Delta H}{a}\right) \quad (8)$$

4. Results and Discussion

Experiments were performed to study the overturning moment of the floating structure in currents; in these experiments, the hydrodynamic pressure was examined in terms of its governing parameters: L/a , e/a , Fr^2 and $\Delta H/a$. The results obtained from the experiments are presented below.

4.1. Shape Ratio of the Floating Structure

The effect of the shape ratio of the floating structure L/a on M_{KP} under $\Delta H/a = 0.10, 0.20, 0.30$ and 0.40 is shown in Figure 5. The behavior, particularly the size and position, is directly related to the overturning moment. The scattered points indicate that under the same $\Delta H/a$, M_{KP} increases significantly with increasing L/a . The values of M_{KP} corresponding to $L/a = 4$ are comparatively larger than that of $L/a = 1, 2$ and 3 . Note that the gradient of growth presents an increasing trend if $\Delta H/a$ is large. The structures' shape increases, resulting in larger surface area under the effect of hydrodynamic pressure and bigger distance to the center point of structures. The higher water level difference results in the higher value of pressure difference. Therefore, the value of M_{KP} is larger and stability is decrease. The relationship between M_{KP} and L/a is linear, and its gradient changes under different $\Delta H/a$. The relationship between M_{KP} and L/a , $\Delta H/a$ is resulted from the variations of hydrodynamics characteristics under different L and ΔH , which are described as follows. During the experiment, with increasing L/a , the flow velocity decreases significantly near the structures' top center. A small recirculation region near the top of the structure expands to the back half of the structure; the minimum pressure value is on the center of the top surface. Larger ratios result in lower pressure on the upper and lower surfaces, and the pressure distribution on the surface is significantly uneven. For a relatively high ratio, the pressure drop is large from the entrance of the bottom gap to the downstream part, causing the increasing pressure difference and giving rise to the overturning moment. Although the larger L partially improves the discharge capacity, the effects of vibration and pressure difference may threaten the safety of the structure. Therefore, it is advisable to increase the safety of the structure by reducing its shape ratio.

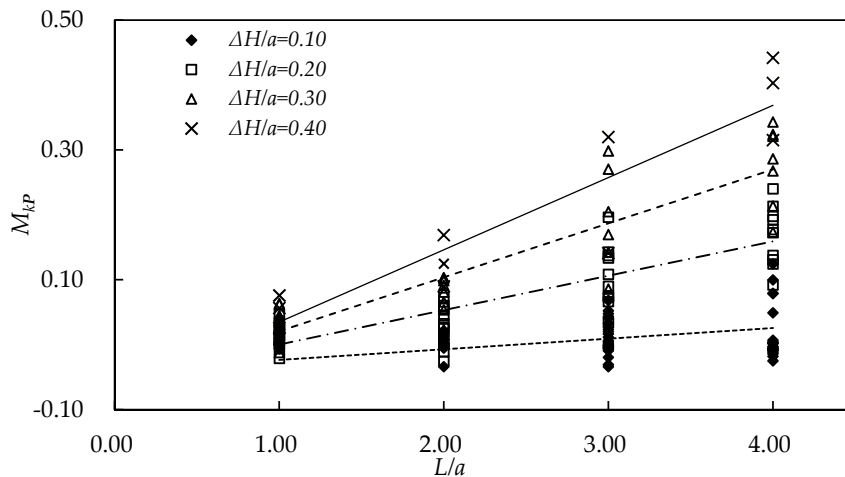


Figure 5. M_{KP} vs. different L/a for $\Delta H/a = 0.10, 0.20, 0.30$ and 0.40 .

Figure 5 shows that M_{KP} increased obviously with the increasing of L/a under the same $\Delta H/a$, and the following equation was obtained

$$M_{KP} = k_1 L/a + c_1 \tag{9}$$

where k_1 is the gradient of growth, and c_1 is a constant term.

The effect of L/a on M_{KP} is different under the influence of $\Delta H/a$. The relationship between M_{KP} and L/a is linear; its gradient of growth k_1 changes under different $\Delta H/a$, and k_1 presents an increasing trend with a larger $\Delta H/a$. A linear relationship is found between the gradient k_1 and $\Delta H/a$:

$$k_1 = k_2 \Delta H/a \tag{10}$$

where k_2 is the coefficient term. Combining Equations (9) and (10), the relationship between M_{KP} and L/a is obtained as follows:

$$M_{KP} = k L/a \times \Delta H/a + c \tag{11}$$

where k is the coefficient term, and c is a constant term.

4.2. Vertical Position

In Figure 6, M_{KP} is plotted against e/a for different values of L/a . The range of M_{KP} shows a decreasing trend with growing e/a in all cases. With increasing e/a , the M_{KP} decreases under the same shape of floating structures. In the same vertical position, larger ratios L/a result in the higher gradient of growth, and this is agreement with the previous conclusion. Hydraulic pressure causes the change of overturning moments in different positions. The hydrodynamic pressure acting on the surface of structures decreases obviously if the floating structure floating upward. For a submerged structure, the hydrostatic pressure results in the pressure distribution and accounts for a large proportion of the total pressure. The distance between the structure's upper edge and the water surface decreases, leading to lower pressure on the surface. Lower pressure reduces the pressure difference, which is an essential cause to reduce M_{KP} . The effect of e/a on M_{KP} is different under the influence of L/a . The relationship between M_{KP} and e/a is linear; its gradient of growth changes under different L/a and presents a linear relationship between them. It is also found that there is the linear relationship between the M_{KP} and e/a and L/a , which is obtained as follows:

$$M_{KP} = k_e L e/a^2 + c_e \tag{12}$$

where k_e is the the coefficient term, and c_e a the constant term.

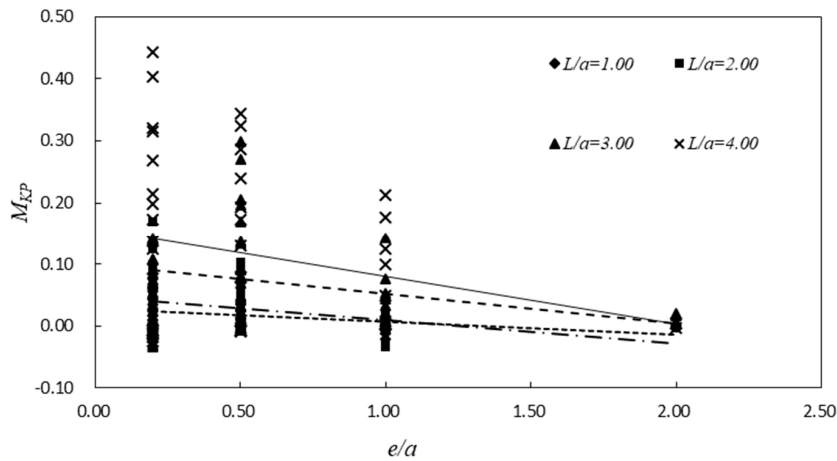


Figure 6. M_{KP} vs. various e/a ratios for $L/a = 1.00, 2.00, 3.00$ and 4.00 .

4.3. Froude Number

In Figure 7, the experimental data of M_{KP} are plotted versus Fr^2 for $L/a = 1.00, 2.00, 3.00$ and 4.00 . The change of the overturning moment is not prominent until Fr^2 reaches 1.00, which is defined as the critical Froude number of the overturning moment. In the range $Fr^2 < 1.00$, L/a influences M_{KP} . The higher shape ratio results in the higher value of M_{KP} and the gradient, in agreement with the previous conclusion. The scattered points indicate that under the same ratio of floating structures, M_{KP} increases significantly with decreasing Fr^2 . If $Fr^2 > 1.00$, then the range of M_{KP} becomes close to a straight line, i.e., L/a has no significant effect on M_{KP} if Fr^2 reaches and exceeds 1.00. Note that the distribution of M_{KP} is wider as L/a grows if Fr^2 is small. M_{KP} and Fr^2 exhibit a nonlinear relationship in all cases. With an increasing velocity, the velocity difference between the upstream and downstream face of the structure becomes larger. Due to the throttling effect of the floating structure, the water level between the upstream and downstream regions increases, leading to an increasing overturning moment and decreasing of its stability. In actual situations, if Fr^2 is lower than its critical value, it has a significant impact on the stability behavior.

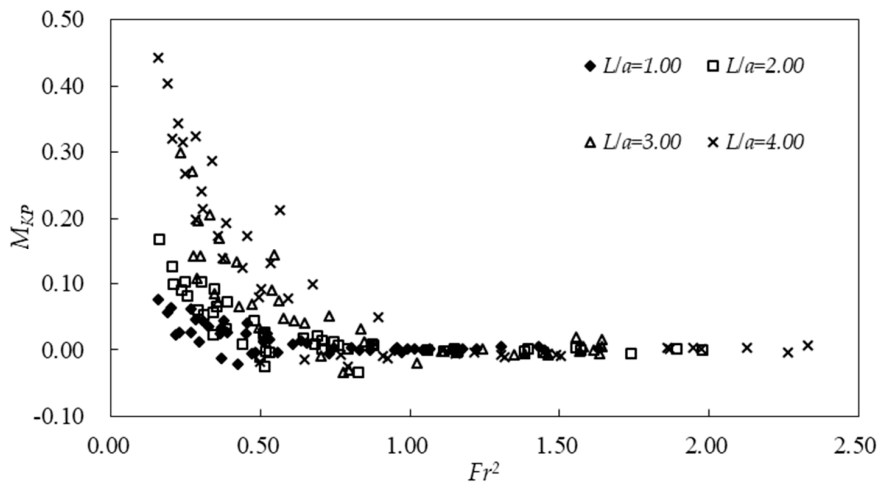


Figure 7. M_{KP} vs. Fr^2 for $L/a = 1.00, 2.00, 3.00$ and 4.00 .

4.4. Water Level

In Figure 8, the effect of $\Delta H/a$ on M_{KP} is shown for all ratios. A greater value of $\Delta H/a$ significantly increases M_{KP} for the same L/a , and with increasing shape ratio, the gradient of M_{KP} becomes larger.

With the increasing water level difference, the hydrodynamic pressure acting on the upstream face of the floating structure is obviously higher than that of downstream face therefore, the structures tilt toward the downstream, and the overturning moment increases obviously. The water flow through the upper surface of structures into the downstream area, the water profile over the floating structure obviously drops, leading to the higher pressure difference. Also, the flow velocity increases significantly under the bigger water level difference. The flow kinetic energy converts to potential energy due to the water acting on the upstream face, resulting in higher hydrodynamic pressure. There is a recirculation zone exists near the downstream face of structures, which causing the lower hydrodynamic pressure acting on downstream face. The overturning moment becomes greater as a result of the pressure distribution under the effect of increasing water level. According to the experimental results, the effect of $\Delta H/a$ on M_{KP} is significant for the same structure. With a higher water level, the instability of the structure increases as a result of the increasing hydrostatic pressure difference between the upstream and downstream faces, and the floating structure becomes easily unbalanced. The effect of $\Delta H/a$ on M_{KP} is different under the influence of L/a . The relationship between M_{KP} and $\Delta H/a$ is linear under same L/a , a linear relationship is found between the gradient of growth and L/a . Equation (11) also can be used to describe the relationship between M_{KP} and $\Delta H/a$: $M_{KP} = k L/a \times \Delta H/a + c$.

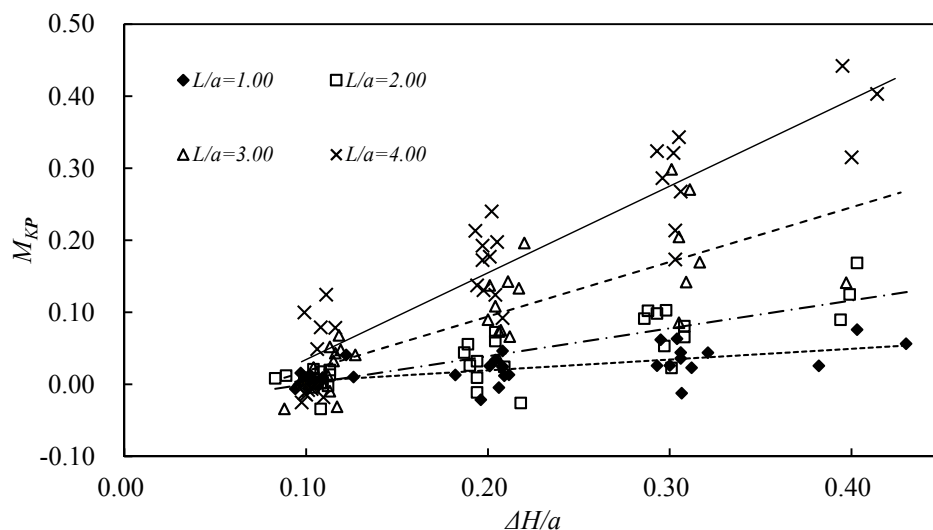


Figure 8. M_{KP} vs. $\Delta H/a$ for $L/a = 1.00, 2.00, 3.00$ and 4.00 .

4.5. Calculation Formula of the Overturning Moment

The formula for M_{KP} is obtained through dimensional analysis. To obtain an equation to describe the relationship of the experimental data, correlation analysis is conducted for the observed data. Compared with nonlinear fitting method, the overturning moment expression obtained by using multiple linear regression analysis has the advantages of simple in form, easy to calculate and more practical in engineering. The scatter plots of Figures 5–8 show that with the same L/a , M_{KP} has a linear correlation with e/a and $\Delta H/a$; the effect of these parameters on M_{KP} is related to L/a if the structure’s shape is change; there is a nonlinear correlation with Fr^2 , the effect of it on M_{KP} is also related to L/a . Ordinary least squares method is a common method for estimating the relationship between the predicted data and the experimental data by minimizing the sum of the squares of the errors. Therefore, the ordinary least squares method is used to fit each parameter for the value of M_{KP} . From dimensionless analysis of Equation (8), a linear algebra relationship between M_{KP} and the variables is expressed as follows:

$$M_{KP} = -0.093 - 0.039 \frac{L}{a} \ln Fr^2 + 0.093 Fr^2 + 0.151 \frac{L \Delta H}{a^2} - 0.003 \frac{Le}{a^2} \tag{13}$$

where M_{KP} and Fr are dimensionless and L , a , ΔH and e are measured in meters. Equation (13) is valid for $H \geq e + a$.

The pressure acting on the floating structure near the sidewall was also measured by taking into account the sidewall effect; the pressure value decreases slightly in a small area near the sidewall. Relative to the pressure acting on the center section, the boundary pressure is essentially unaffected. In actual situations, it is reasonable to calculate the overturning moment using the pressure acting on the central section.

5. Verification and Error Analysis

To evaluate the accuracy of the estimate Equation (13), the adjusted multiple correlation coefficients (AMCC) and the standard error of estimation (SEE) were used. AMCC is the modified version of the multiple correlation coefficients; it gives the percentage of variation explained by only those significant variables that in reality affect the predicted value. The value of AMCC indicates the goodness of the fit of the M_{KP} values, it was used to verify the prediction is right and the regression model is satisfactory. The value of SEE evaluates the reliability of the data, smaller values are better, which indicates that the observations are closer to the fitted line. The quantities of AMCC and SEE are defined as follows:

$$R^2 = \frac{\sum_{k=1}^K (\tilde{y}_k - \bar{y})^2}{\sum_{k=1}^K (y_k - \bar{y})^2} \quad (14)$$

$$\text{AMCC} = R^2 - \frac{J \times (1 - R^2)}{K - J - 1} \quad (15)$$

$$\text{SEE} = \sqrt{\frac{\sum_{k=1}^K (y_k - \tilde{y}_k)^2}{K - J - 1}} \quad (16)$$

where R^2 is the coefficient of determination, K is the size of the data set, J is the number of dimensionless independent variables, and y_k is the measured value of M_{KP} . Here, \tilde{y}_k is the estimated value of M_{KP} of Equation (13), and \bar{y} is the mean value of y_k .

It is determined that AMCC and SEE for Equation (13) are 0.90 and 0.02, respectively, thus proving that the significance is strong.

The model can be further tested to judge its applicability of the regression equation and the fitting effect. A 95% confidence interval was selected; the corresponding value of F is 395.10. Autocorrelation affects the ability to conduct valid statistical tests. Autocorrelation affects the ability to conduct valid statistical tests. The autocorrelation of the model was evaluated by using Dubin-Watson (DW) test which is commonly used. The significance test of variables is meaning and the prediction of the model is valid if the value of DW is smaller than 5. The value of DW was 1.84, that is, no autocorrelation exists in the model. The correlation coefficient of the formula between the variables is low; the independent variables are not correlated. Multicollinearity produces large standard errors in the related independent variables and it causes imprecise estimates of coefficient values, it also results in the imprecise and instability the model predictions. To quickly eliminate the instability of the model, the variance inflation factor (VIF) method was used to perform multicollinearity diagnosis. The maximum value of VIF was 5.60; thus, there is no multicollinearity problem between the variables and M_{KP} . The F -test, DW test and VIF test formulas are given as follows:

$$F = \frac{\sum_{k=1}^K (\tilde{y}_k - \bar{y}_k)^2 / K}{\sum_{k=1}^K (y_k - \tilde{y}_k)^2 / (K - J - 1)} \quad (17)$$

$$\text{DW} = \frac{\sum_{t=1}^K (e_t - e_{t-1})}{\sum_{t=2}^K e_t^2} \quad (18)$$

$$\text{VIF}_i = (1 - R_i^2)^{-1} \quad (19)$$

where \bar{y}_k is the mean value of \tilde{y}_k , e_t is the error term at time t , and R_i^2 is the multiple coefficient of determination of the independent variable.

The standard residuals need to satisfy the requirements of randomness and normality to prove the correctness of the obtained formula. The following results were obtained by analyzing the standard residuals. Figure 9 illustrates the corresponding statistical analysis of the residuals of Equation (13) and the histogram of the residuals with normal probability curve; the residuals present a normal distribution. The 95% distribution of standardized residual is between -2 and $+2$, which suggests that the model assumptions are reasonable. Figure 10 shows the scatter plot of the standardized residual.

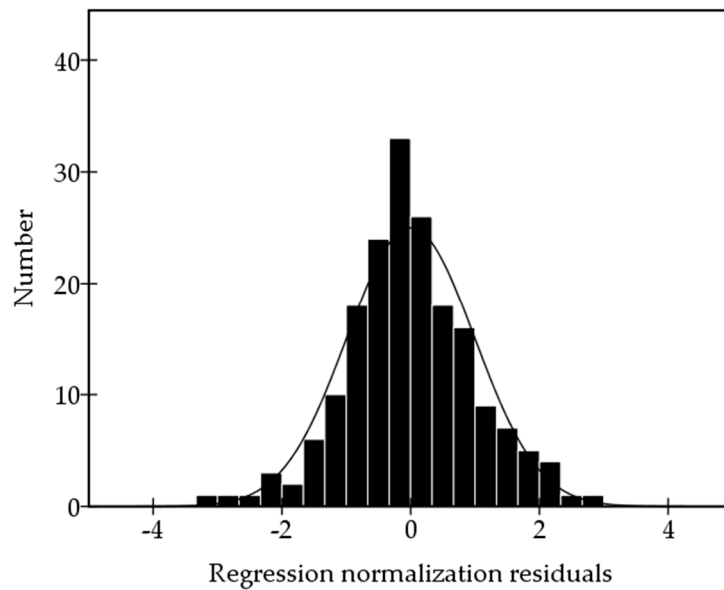


Figure 9. Residual distribution histogram.

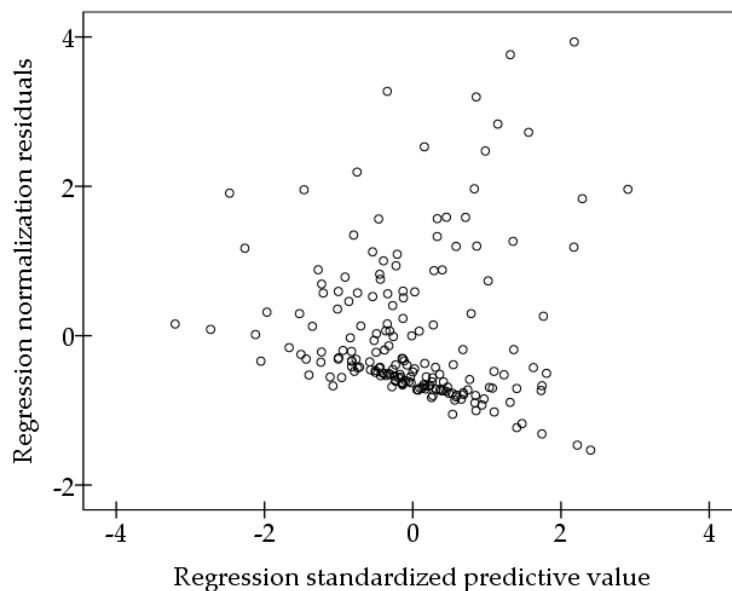


Figure 10. Scatter plot of standardized residual (mean = 0, standard deviation = 0.989, N = 186).

As for M_{KP} , the comparison between the measured and calculated results is shown in Figure 11, suggesting a good agreement. Thus, the calculation formula of overturning moment is obtained.

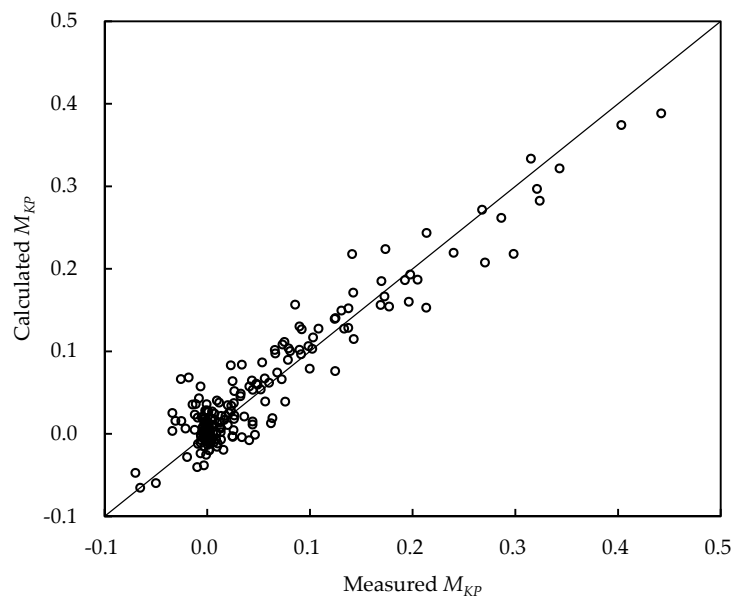


Figure 11. Comparison between the measured and calculated values of M_{KP} .

6. Conclusions

The overturning moment of the floating structure influenced by currents was assessed by means of theoretical analysis and physical model tests. A calculation formula was proposed by using dimensional analyses between the overturning moments and the contributing parameters: structural shape ratios, structural vertical positions, flow velocities and water levels.

The structure shape ratio influences the stability of the structure. The stability deteriorates as the ratio increases; the range of overturning moment shows a decreasing trend with the increase of structural vertical positions. The stability of structures is influenced by Fr^2 . If the value of Fr^2 is small (≤ 1), then the overturning moment decreases significantly with increasing Fr^2 . If the Fr^2 value is greater than 1, then the range of overturning moment converges to a straight line, and the effect of Fr^2 on overturning moment is not easily detectable. A lower water level leads to smaller overturning moment and improves the stability of structures.

Nonlinear regression and multi-linear regression were used to obtain the formula for calculation of the overturning moment. Statistical indices were used to quantitatively investigate the accuracy of the formula; the values of AMCC and SEE were 0.90 and 0.02, respectively, and the residuals of the formula presented normal distribution. The calculation formula is in agreement with the experimental data, thus supporting the validity of the stability evaluation. Compared with the action of hydrodynamic pressure, the role of shear force is small. This study did not consider overturning generated by shear stress; In order to study the systematical and accurate value of overturning moment in prototype engineering, the moment and the proportion generated by shear force can be studied in the future. Thus, the influence of shear stress on the overturning phenomenon and its proportion are recommended for evaluation in the future.

Acknowledgments: The authors acknowledge the financial support provided by the National Key R & D Program of China (2016YFC0402501), the National Natural Science Foundation of China (Grant No. 51279048), the Fundamental Research Funds for the Central Universities (2016B40414), the 111 Project (B17015, B12032) and the Priority Academic Program Development of Jiangsu Higher Education Institutions (YS11001).

Author Contributions: Z.F. conceived and designed the experiments; Z.C. performed the experiments, analyzed the data and wrote the paper. W.D. and Z.L. improved the quality of the paper. The authors also thank Hanqing Zhao, Haitong Zhang and James Yang, who works in Hydraulic Engineering Department, KTH Royal Institute of Technology, for their valuable comments, which significantly improved the quality of the paper.

Conflicts of Interest: The authors declare no conflict of interest.

References

- Olyaie, E.; Banejad, H.; Chau, K.; Melesse, A.M. A comparison of various artificial intelligence approaches performance for estimating suspended sediment load of river systems: A case study in United States. *Environ. Monit. Assess.* **2015**, *187*, 189. [[CrossRef](#)] [[PubMed](#)]
- Wang, W.; Xu, D.; Chau, K.; Lei, G. Assessment of river water quality based on theory of variable fuzzy sets and fuzzy binary comparison method. *Water Resour. Manag.* **2014**, *28*, 4183–4200. [[CrossRef](#)]
- Gholami, V.; Chau, K.W.; Fadaee, F.; Torkaman, J.; Ghaffari, A. Modeling of groundwater level fluctuations using dendrochronology in alluvial aquifers. *J. Hydrol.* **2015**, *529*, 1060–1069. [[CrossRef](#)]
- Chau, K. Use of Meta-Heuristic Techniques in Rainfall-Runoff Modelling. *Water* **2017**, *9*, 186. [[CrossRef](#)]
- Albano, R.; Sole, A.; Mirauda, D.; Adamowski, J. Modelling large floating bodies in urban area flash-floods via a Smoothed Particle Hydrodynamics model. *J. Hydrol.* **2016**, *541*, 344–358. [[CrossRef](#)]
- Chen, L.F.; Sun, L.; Zang, J.; Hillis, A.J.; Plummer, A.R. Numerical study of roll motion of a 2-D floating structure in viscous flow. *J. Hydrodyn. Ser. B* **2016**, *28*, 544–563. [[CrossRef](#)]
- Fu, Z.F.; Yan, Z.M. Stability analysis on a new type of floating sluice. *J. Hydraul. Eng.* **2005**, *8*, 1014–1018. [[CrossRef](#)]
- Roy, P.D.; Ghosh, S. Wave force on vertically submerged circular thin plate in shallow water. *Ocean Eng.* **2006**, *33*, 1935–1953. [[CrossRef](#)]
- Seiffert, B.; Hayatdavoodi, M.; Ertekin, R.C. Experiments and computations of solitary-wave forces on a coastal-bridge deck. Part I: Flat plate. *Coast. Eng.* **2014**, *88*, 194–209. [[CrossRef](#)]
- Hayatdavoodi, M.; Seiffert, B.; Ertekin, R.C. Experiments and computations of solitary-wave forces on a coastal-bridge deck. Part II: Deck with girders. *Coast. Eng.* **2014**, *88*, 210–228. [[CrossRef](#)]
- Hayatdavoodi, M.; Ertekin, R.C. Wave forces on a submerged horizontal plate—Part I: Theory and modelling. *J. Fluid Struct.* **2015**, *54*, 566–579. [[CrossRef](#)]
- Hayatdavoodi, M.; Ertekin, R.C. Wave forces on a submerged horizontal plate—Part II: Solitary and cnoidal waves. *J. Fluid Struct.* **2015**, *54*, 580–596. [[CrossRef](#)]
- Lee, S.M.; Hong, C.B. Characteristics of wave exciting forces on a very large floating structure with submerged plate. *J. Mech. Sci. Technol.* **2005**, *11*, 2061–2067. [[CrossRef](#)]
- Belibassakis, K.A.; Athanassoulis, G.A. A coupled-mode technique for weakly nonlinear wave interaction with large floating structures lying over variable bathymetry regions. *Appl. Ocean Res.* **2006**, *28*, 59–76. [[CrossRef](#)]
- Liu, C.F.; Teng, B.; Gou, Y.; Sun, L. A 3D time-domain method for predicting the wave-induced forces and motions of a floating body. *Ocean Eng.* **2011**, *38*, 2142–2150. [[CrossRef](#)]
- Hadžić, I.; Hennig, J.; Peric, M.; Xing-Kaeding, Y. Computation of flow-induced motion of floating bodies. *Appl. Math. Model.* **2005**, *29*, 1196–1210. [[CrossRef](#)]
- Zhou, B.Z.; Wu, G.X.; Meng, Q.C. Interactions of fully nonlinear solitary wave with a freely floating vertical cylinder. *Eng. Anal. Bound. Elem.* **2016**, *69*, 119–131. [[CrossRef](#)]
- Xing, D.L.; Deng, Y.P.; Zhou, M. Experimental research for added mass of cylinders with reflected boundary condition. *J. Dalian Univ. Technol.* **1998**, *38*, 107–111. [[CrossRef](#)]
- Xing, D.L. Research on hydrodynamic performance of floating bodies in confined zone. *J. Dalian Univ. Technol.* **1993**, *3*, 351–355. [[CrossRef](#)]
- Lu, Y. Stability Analysis and Experimental Study of Large Floating Box Door in Dynamic Water. Master's Thesis, Hohai University, Nanjing, China, 2002.
- Fu, Z.F.; Yin, X.J.; Gu, X.F. Hydraulic characteristics of floating sluices subsiding and buoying in flowing water. *Adv. Sci. Technol. Water Resour.* **2014**, *34*, 24–27. [[CrossRef](#)]
- Huang, S.Q.; Huang, S.F.; Huang, G.F.; Xu, J. The research on numerical simulation of on-off process of floating sluice in dynamic water. In Proceedings of the 23rd National Symposium on Water Dynamics and the 10th National Symposium on Water Dynamics, Xi'an, China, 19–24 September 2011; p. 7.
- Fan, B.Q.; Suo, L.S.; Zhou, J. Analysis of floating structures for tidal power houses. *Water Conserv. Hydropower Sci. Technol. Prog.* **2002**, *22*, 20–22.
- Fan, B.Q.; Suo, L.S. Floating Stability Calculation of Floating-caisson of Tidal Power Plants. *Water Conserv. Hydropower Sci. Technol. Prog.* **2000**, *3*, 49–52.

25. Johnson, H.K.; Karambas, T.V.; Avgeris, I.; Zanuttigh, B.; Gonzalez-Marco, D.; Caceres, I. Modelling of Waves and Currents around Submerged Breakwaters. *Coast. Eng.* **2005**, *52*, 949–969. [[CrossRef](#)]
26. Rey, V.; Touboul, J. Forces and moment on a horizontal plate due to regular and irregular waves in the presence of current. *Appl. Ocean Res.* **2011**, *33*, 88–99. [[CrossRef](#)]
27. Karmakar, D.; Guedes Soares, C. Scattering of gravity waves by a moored finite floating elastic plate. *Appl. Ocean Res.* **2012**, *34*, 135–149. [[CrossRef](#)]
28. Cui, Z.; Fu, Z.; Chen, Y. Explore the flow characteristics of floating structure based on the orthogonal design method. *J. Wuhan Univ. (Eng. Ed.)* **2018**. accepted.
29. Zhen, C.; Zongfu, F.; Yuejun, C.; Shan, W.; Guanggang, M.; Wen, J. Explore the hydrodynamic force on the surface of floating structure in finite flowing water. In Proceedings of the 37th International Association for the History of Religions (IAHR) World Congress, Kuala Lumpur, Malaysia, 13–18 August 2017.



© 2018 by the authors. Licensee MDPI, Basel, Switzerland. This article is an open access article distributed under the terms and conditions of the Creative Commons Attribution (CC BY) license (<http://creativecommons.org/licenses/by/4.0/>).